31st Annual International Conference of the IEEE EMBS
Minneapolis, Minnesota, USA, September 2-6, 2009

Identification of Small World Topologies in Neural Functional Connections Quantified by Phase Synchrony Measures

Marcos E. Bolaños, Edward M. Bernat, and Selin Aviyente

Abstract— **The brain is a complex biological system with dynamic interactions between its sub-systems. One particular challenge in the study of this complex system is the identification of dynamic functional networks underlying observed neural activity. Current imaging approaches index local neural activity very well, but there is an increasing need for methods that quantify the interaction between regional activations. In this paper, we focus on inferring the functional connectivity of the brain based on electroencephalography (EEG) data. The interactions between the different neuronal populations are quantified through a recently proposed dynamic measure of phase synchrony. Small world measures, which include clustering coefficient, path length, global efficiency, and local efficiency, are computed on graphs obtained through the phase synchrony measure to study the underlying functional networks. The proposed measures are applied to an EEG study containing the error-related negativity (ERN), a brain potential response that indexes endogenous action monitoring, to determine the organization of the brain during a decision making task and determine the differences between Error and Correct responses.**

I. INTRODUCTION

The brain follows two organizational principles referred to as functional segregation and functional integration, enabling the rapid extraction of information and the generation of coherent brain states [1]. Any mechanism for neural integration must involve interactions between the functionally relevant local networks. To examine functional integration in the temporal frame, there is a need to characterize the temporal dynamics of neural networks with millisecond accuracy. Neurophysiological measures with high temporal resolution, such as the electroencephalogram (EEG), are the most appropriate tools for examining the dynamic interactions of neural networks.

Types of indices used for quantifying functional connectivity include linear measures, such as correlation and coherence, and nonlinear measures, such as phase synchrony and generalized synchronization measures [2]. Phase synchrony is a particularly attractive measure for quantifying the connectivity since it is believed that networks of reciprocal interactions are key to integration. In recent work [3], we have proposed a new time-varying measure of phase synchrony that quantifies the dynamic nature of the interactions between neuronal oscillations with a high time-frequency resolution.

Although phase synchrony measures are effective at quantifying the pairwise interactions between neuronal populations, they do not reveal much information about the overall organization of the brain. Previous MRI [4], MEG [5], and EEG [6] studies have applied graph theoretical measures on neurophysiological data for understanding the organization of the brain. In particular, small world network topology has been used to understand the functioning of neural networks. The main motivation behind using small world theory is that high clustering coefficients and short path lengths observed in small world networks are analogous to the principles of functional segregation and integration in the brain.

The study presented here utilized data from an electroencephalography experiment, which consisted of error-related negativity (ERN), to determine the organization of the brain during a decision making task and identify differences between Error and Correct responses.

II. NEURAL SYNCHRONIZATION AND FUNCTIONAL INTEGRATION MEASURES

A. Time-Frequency Phase Synchrony

In recent work, we have introduced a new time-varying measure of phase synchrony based on a complex-valued time-frequency distribution introduced by Rihaczek [7]. For a signal, $x(t)$, Rihaczek distribution is expressed as

$$C(t,\omega) = \frac{1}{\sqrt{2\pi}} x(t) X^*(\omega) e^{-j\omega t} \tag{1}$$

and measures the complex energy of a signal at time t and frequency ω.

One of the disadvantages of Rihaczek distribution is the existence of cross-terms for multicomponent signals. In order to get rid of these cross-terms, we introduced a reduced interference version of Rihaczek distribution by applying a kernel function such as the Choi-Williams (CW) kernel [8] with $\phi(\theta,\tau) = \exp(\frac{-(\theta\tau)^2}{\sigma})$ to filter the cross-terms to obtain

$$C(t,\omega) = \iint e^{\left(\frac{-(\theta\tau)^2}{\sigma}\right)} e^{\left(j\frac{\theta\tau}{2}\right)} A(\theta,\tau) e^{-j(\theta t+\tau\omega)} d\tau d\theta \tag{2}$$

where $A(\theta,\tau) = \int s(u+\frac{\tau}{2}) s^*(u-\frac{\tau}{2}) e^{j\theta u} du$ is the ambiguity function of the signal and $exp(j\theta\tau/2)$ is the kernel corresponding to the Rihaczek distribution [7]. This new distribution satisfies the marginals and preserves the energy, and is a complex energy distribution at the same time. The

This work was in part supported by the National Science Foundation under Grants No. CCF-0728984, CAREER CCF-0746971.

M. E. Bolaños (bolanosm@msu.edu) and S. Aviyente (aviyente@egr.msu.edu) are with the Department of Electrical Engineering, Michigan State University, 2120 Engineering Building, East Lansing, MI, 48824, USA.

E. M. Bernat is with the Department of Psychology, University of Minnesota, 75 East River Road, Elliot Hall, Minneapolis, MN, 55455, USA.

value of σ can be adjusted to achieve a desired trade-off between resolution and the amount of cross-terms retained. We can compute the phase difference between two signals based on this complex distribution as

$$\Phi_{12}(t,\omega) = \arg\left[\frac{C_1(t,\omega)C_2^*(t,\omega)}{|C_1(t,\omega)||C_2(t,\omega)|}\right] \quad (3)$$

and can define a synchrony measure based on quantifying the intertrial variability of the phase differences, named the phase locking value (PLV)

$$PLV(t,\omega) = \frac{1}{N}\left|\sum_{k=1}^{N}\exp(j\Phi_{12}^k(t,\omega))\right| \quad (4)$$

where N is the number of trials and $\Phi_{12}^k(t,\omega)$ is the time-varying phase estimate between two electrodes for the kth trial. If the phase difference varies little across the trials, PLV is close to 1.

B. Graph Theoretic Measures

A graph G is defined by $(V_G, E_G, \Re_G)$ where V_G is a set of vertices, E_G is a set of edges, and $\Re_G$ is an incident function that associates with each edge a pair of vertices. The graphs in this study are simple and undirected binary graphs.

After G is obtained, a distance matrix, D, is required for calculating various graph measures. D contains the number of edges required to link each pair of vertices in the graph. If a path does not exist between two vertices, the distance is assigned as 0. The distance matrix is acquired by generating G^r for $1 \le r \le N-1$. $D_{ij} = r$ if the first non-zero integer appears in G_{ij}^r. Once G and D are obtained, one can compute the major parameters to identify the global organization of the network such as average degree, K_G, clustering coefficient, C_G, path length, L_G, global efficiency, E_G^{global}, and local efficiency, E_G^{local}.

The clustering coefficient quantifies the level of functional integration in the network. C_i represents the ratio of the existing connections between neighbors of v_i and all possible connections. It is calculated by identifying all neighbors of v_i, m_i, followed by identifying how many edges, $|E_{G_i}|$, are shared among the neighbors. The maximum possible pairs of neighbors sharing edges is calculated as $|E_{G_i}^{max}| = \binom{|m_i|}{2}$. The clustering coefficient of a particular node is

$$C_i = \frac{|E_{G_i}|}{|E_{G_i}^{max}|} \quad (5)$$

and the clustering coefficient for the graph, C_G, is the average of C_i over all nodes.

The characteristic path length of the brain quantifies its functional segregation. L_i of v_i is calculated by the average distance required to reach each of the other vertices in the graph and is equal to

$$L_i = \frac{1}{n_i}\sum_{j=1}^{N} D_{i,j} \quad (6)$$

where n_i is the number of non-zero distances between v_i and v_j. The characteristic path length for the entire graph, L_G, is the average of all L_i.

Global and local efficiencies give indication on how efficient information is transmitted throughout the network [9]. Typically, C and L can be used to estimate the local and global efficiencies respectively. A graph's global efficiency is inversely related to the shortest distance available to transmit the information from v_i to v_j. From [10], the global efficiency is

$$E^{global} = \frac{1}{N^2 - N}\sum_{i\neq j\in G}\frac{1}{D_{i,j}}. \quad (7)$$

The local efficiency is similar to global efficiency defined for each node and can be understood as a measure of the fault tolerance of the network, indicating how well each subgraph, G_i, exchanges information when v_i is removed from G. The local efficiency is given by

$$E_i^{local} = \frac{1}{{N_{G_i}}^2 - N_{G_i}}\sum_{j\neq k\in G_i}\frac{1}{D_{j,k}}. \quad (8)$$

An overall local efficiency for the graph was calculated by averaging all E_i^{local}.

In order to evaluate the small world behavior of G, its parameters need to be compared to random graphs. The random graphs used for this study were generated using an algorithm [11] where connections between vertices were assigned with uniform probability of $P(G_{i,j}^{rand} = 1) = \frac{Q}{N^2-N}$ where Q is the number of edges in G. Similarly, lattice graphs were generated by assigning k connections to adjacent vertices where $1 \le k \le N-1$. G is characterized as a small world network if $\gamma = \frac{C_G}{C_{rand}} \gg 1$ and $\lambda = \frac{L_G}{L_{rand}} \approx 1$ [12]. A measure of small worldness is identified as $\sigma = \frac{\gamma}{\lambda}$ where $\sigma \gg 1$ reveals the existence of a small world topology within the graph.

III. Data

A. Error Related Negativity

The phase synchrony measure was applied to a set of EEG data containing the error-related negativity (ERN). The ERN is a brain potential response that occurs following performance errors in a speeded reaction time task. The ERN has been characterized as a neurophysiological index of endogenous action monitoring-the automatic capacity to monitor behavioral performance on-line and to initiate corrective action as needed, either through detection of errors [13] or detection of conflict among competing neural response pathways [14]. Our previous work indicates that there is increased phase synchrony associated with ERN for the theta frequency band for Error responses compared to Correct responses [3].

B. Test Subjects

EEG data from 63-channels was collected from 84 undergraduate students (34 male) from the University of Minnesota. Recordings were done in accordance with the 10/20

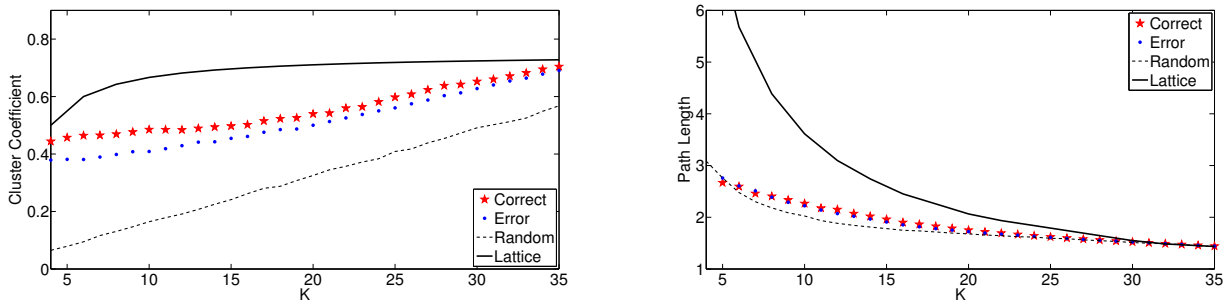

(a) (b)

Fig. 1: a) Plot of mean clustering coefficients, C, derived from correct (star) and error (circle) groups. b) Plot of mean path lengths, L, derived from correct (star) and error (circle) groups. L and C for lattice (solid line) and random (dashed line) graphs are plotted for comparison. Data is plotted with respect to average degree, K.

system on a Neuroscan Synamps2 system (Neuroscan, Inc.). A speeded-response flanker task was employed, and error and correct response-locked averages were computed for each subject.

C. Baseline Correction

Phase synchrony measures represent the actual phase difference between two signals for a defined time and frequency. In order to more accurately measure transient changes in phase-synchrony (instead of constant synchrony), we baseline corrected the time-frequency phase-synchrony values. We chose a baseline before the initial stimulus was delivered (-990 to -900 ms). Baseline correction is applied by subtracting the average phase synchrony at each frequency for the pre-stimulus time range post-stimulus phase synchrony as follows:

$$PLV_c(t,\omega) = PLV(t,\omega) - \frac{1}{|\text{Length of pre-stimulus}|}\sum_{t\in pr.s.} PLV(t,\omega). \quad (9)$$

IV. Results

A. Connectivity Matrix

Eighty-four 63x63 connectivity matrices containing the baseline corrected average phase synchrony values in the theta frequency band (4-7 Hz) and ERN time window (25-75 ms) for each electrode pair from the 10/20 arrangement were generated for Error and Correct responses.

B. Adjacency Matrix

The phase synchrony matrices were converted into undirected binary graphs, G, by applying a threshold, T. Through this method, pairs of electrodes with phase synchrony values greater or equal to the threshold were designated a 1 and those below the threshold a 0. A range of T were applied to the graphs in intervals of 0.001 for $\alpha \leq T \leq \beta$ where α and β are the minimum and maximum phase synchrony values within the entire set of subject groups, respectively. The four specified graph measures were then implemented and computed with respect to average degree, K_G.

C. Clustering Coefficient and Path Length

From Fig. 1a, it can be seen that as K_G increases, C_{error} and $C_{correct}$ remain greater than C_{rand}, i.e. the human brain is more clustered compared to a random network. Fom Fig. 1b it is seen that L_{error} and $L_{correct}$ are approximately equal to L_{rand}. Comparing the two subject groups to each other using a one tailed t-test, $C_{correct} > C_{error}$ ($p < 10^{-12}$) for $4 \leq K \leq 35$ indicating a decrease in functional integration during Error responses. Also, a significant difference between the two subject groups occurs for $9 \leq K \leq 35$ where $L_{error} < L_{correct} (p < 10^{-5})$. This is indicative of a decrease in functional segregation during Error responses.

D. Global Efficiency and Local Efficiency

From Fig. 2a and 2b, it can be seen that local and global efficiency show a significant difference between the two subject groups for $4 \leq K \leq 35$. A t-test revealed $E^{local}_{correct} > E^{local}_{error}$ ($p < 10^{-12}$). This indicates that the efficient transmission of information among locally clustered nodes degenerates for error responses compared to correct responses. Local efficiency was expected to give indications of significant changes between the two subject groups just as clustering coefficient had since clustering coefficient can be regarded as the local efficiency of information transmission within the neighborhood of each individual vertex, e.g. [9] uses clustering coefficient as a close approximation for local efficiency.

A one tailed t-test on the global efficiency revealed $E^{global}_{correct} < E^{global}_{error}$ ($p < 10^{-4}$) for $4 \leq K \leq 14$. For $15 \leq K \leq 35$, $E^{global}_{error} < E^{global}_{correct}$ ($p < 0.01$). This indicates that the efficient transmission of information globally degenerates during Correct responses when the graphs are very sparse. By observing the behavior of path length as compared to global efficiency, path length can be used as a close approximation for global efficiency through an inverse relationship.

E. Small World Measures

The first observation from Fig. 3c is that $\sigma_{correct} >> 1$ and $\sigma_{error} >> 1$ indicating the brain performs as a small world network. Secondly, the figure shows that the small world

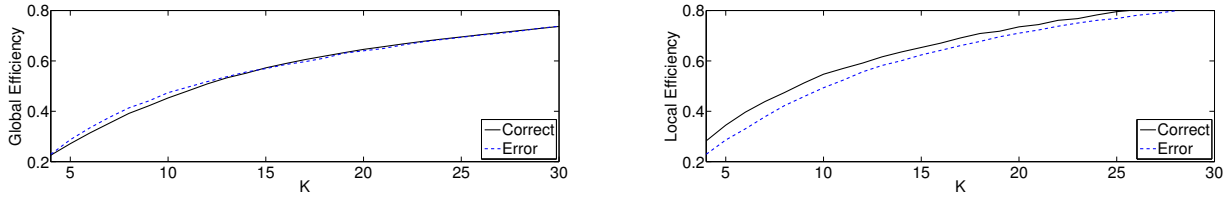

(a) (b)

Fig. 2: a) Plot of correct (solid line) and error (dashed line) global efficiencies with respect to average degree, K. b) Plot of correct (solid line) and error (dashed line) local efficiencies with respect to average degree, K.

topology of the brain decreased during Error responses for $4 \leq K \leq 20$. A one tailed t-test revealed $\sigma_{error} < \sigma_{correct}$ ($p < 10^{-4}$). It is also observed that clustering coefficient has a stronger influence on the decrease in small world topology compared to the path length. This indicates that the brain is organized more like a small network for the Correct responses compared to the Error responses where functional integration diminished.

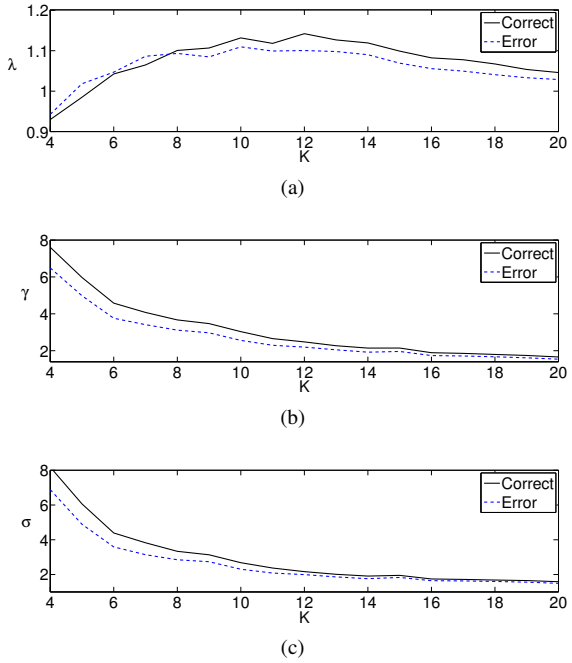

(a) (b) (c)

Fig. 3: a) Plot of λ with respect to average degree, K. b) Plot of γ with respect to average degree, K. c) Plot of small world measure, σ, with respect to average degree, K. Correct plotted with solid line/Error plotted with dashed line.

V. Conclusion

In this paper, we applied global graph theoretic measures to study the small world topology of the brain associated with ERN. The results of this study, in concordance with previous studies, shows that the brain follows a small world topology when processing visual stimulus. We have also observed significant decreases in local efficiency and clustering during Error responses compared to Correct responses, indicating loss of the optimal organization normally expected in the brain. Future work will focus on identifying the local networks of the brain by determining hubs and functional modules within the network.

References

[1] O. Sporns, D. R. Chivalo, M. Kaiser, and C. C. Hilgetag, "Organization, development and function of complex brain networks," in *Trends in Cognitive Sciences*, vol. 8, no. 9, 2004, pp. 418–425.

[2] E. Pereda, R. Rial, A. Gamundi, and J. Gonzales, "Assessment of changing interdependencies between human electroencephalograms using nonlinear methods," in *Physica D*, vol. 148, 2001, pp. 147–158.

[3] S. Aviyente, E. M. Bernat, W. S. Evans, C. J. Patrick, and S. R. Sponheim, "A phase synchrony measure for quantifying dynamic functional integration in the brain," *Submitted for Publication*, 2008.

[4] K. Supekar, V. Menon, D. Rubin, M. Musen, and M. D. Greicius, "Network analysis of intrinsic functional brain connectivity in alzheimer's disease," in *Computational Biology*, vol. 4, 2008, pp. 1–11.

[5] C. J. Stam, "Functional connectivity patterns of human magnetoencephalographic recordings: A 'small-world' network?" in *Neuroscience Letters*, vol. 355, 2003, pp. 25–28.

[6] C. J. Stam, B. F. Jones, G. Nolte, M. Breakspear, and P. Scheltens, "Small-world networks and functional connectivity in alzheimer's disease," in *Cerebral Cortex Advance Access*, vol. 17, 2006, pp. 92–99.

[7] A. Rihaczek, "Signal energy distribution in time and frequency," in *IEEE Transactions: Information Theory*, vol. 14, 1968, pp. 369–274.

[8] H. Choi and W. J. Williams, "Improved time-frequency representation of multicomponent signals using exponential kernels," in *IEEE Transactions on Acoustics*, vol. 17, no. 6, 1989, pp. 862–871.

[9] V. Latora and M. Marchiori, "Efficient behavior of small-world networks," in *Physical Review Letters*, vol. 87, no. 19, 2001, p. 198701.

[10] S. Achard and E. Bullmore, "Efficiency and cost of economical brain functional networks," in *PLos Computational Biology*, 2007.

[11] O. Sporns and J. D. Zwi, "The small world of the cerebral cortex," in *Neuroinformatics*, vol. 2, no. 2, 2004, pp. 145–162.

[12] D. J. Watts and S. H. Strogatz, "Collective dynamics of 'small-world' networks," *Nature*, vol. 393, no. 4, pp. 440–442, 1998.

[13] W. J. Gehring, M. G. Coles, D. E. Meyer, and E. Donchin, "A brain potential manifestation of error-related processing," in *Electroencephalograph Clin*, vol. 44, no. 261-272, 1995.

[14] C. S. Carter, T. S. Braver, D. M. Barch, M. M. Botvinick, D. Noll, and J. D. Cohen, "Anterior cingulate cortex, error detection, and the online monitoring of performance," in *Science*, vol. 280(5364), 1998.